Deep Learning-based MISO-NOMA-HBF-BFNN to Improve Channel Capacity for B5G

Md Shoriful Islam[1], Ahmed Al Amin[2], and Muhammad Atique Masud[3]

[1]Brigham Young University
[2]University of Michigan-Dearborn Department of Electrical and Computer Engineering
[3]Uttara University

August 30, 2023

Turk J Elec Eng & Comp Sci
() : –

Deep Learning-based MISO-NOMA-HBF-BFNN to Improve Channel Capacity for B5G

Ahmed Al Amin PhD[1]*, Md Shoriful Islam[2], Muhammad Atique Masud[3]
[1]Department of Electrical and Computer Engineering, University of Michigan, Dearborn, Michigan, 48128, USA,
ORCID iD: https://orcid.org/0000-0002-4093-6810
[2]Department of Electrical and Computer Engineering, Brigham Young University, Utah, 84602, USA,
[3]Department of Electrical Engineer, Uttara University, Dhaka, 1230, Bangladesh,

Received: .202 • **Accepted/Published Online:** .202 • **Final Version:** ..202

[1]

Abstract: In this study, multiple-input single-output based non-orthogonal multiple access (MISO-NOMA) with hybrid beamforming (HBF) (MISO-NOMA-HBF) and beamforming neural network (BFNN) for cell edge user (CEU) are integrated (termed as MISO-NOMA-HBF-BFNN) for mmWave based beyond 5G cellular communication system to support multiple users simultaneously and provide significantly improved user channel capacities and sum channel capacity (SC) as well. Simulation results illustrated the effectiveness of the proposed MISO-NOMA-HBF-BFNN scheme over the existing MISO-NOMA with HBF and MISO-OMA with HBF-BFNN based schemes in case of user capacities and SC as well.

Key words: Beamforming neural network, beyond 5G, deep learning, hybrid beamforming, non-orthogonal multiple access, sum capacity, user capacity.

1. Introduction

Recently, the research community has paid attention to non-orthogonal multiple access (NOMA) for providing multiple users with an ample data rate [1]. A number of studies have been conducted on increasing the channel capacity for the power domain downlink NOMA [1-2]. By utilizing the successive interference cancellation (SIC) technique, a user with good channel conditions can decode their corresponding signal while direct decoding can be performed on the user side with relatively worse channel conditions. Due to the limited number of resources (time/frequency/code), existing orthogonal multiple access (OMA) techniques (TDMA/FDMA/CDMA) can face severe challenges when used beyond 5G (B5G) cellular communication systems [3]. Additional resource utilization can degrade the user capacities as well as the sum capacity (SC) of OMA-based cellular communication systems which can be overcome by the power domain NOMA. Moreover, NOMA and millimeter wave (mmWave) provide a solution for B5G cellular communication because mmWaves can provide ultra-high channel capacities and NOMA can simultaneously support multiple access for multiple users [4]. So, a suitable multiuser, high user capacity, and imperfect channel state information (CSI) based solution for mmWave based B5G cellular communication is required. Moreover, multiple-input-single-output-based hybrid beamforming

*Correspondence: shaon04@gmail.com

The pre-print is available at 10.22541/au.168016142.28646747/v1

(MISO-HBF) is a suitable solution for mmWave systems [13]. But the narrow beam channel provides coverage for a single user in the case of the conventional MISO-HBF scheme. To provide the multiuser access of the conventional MISO-HBF based scheme, NOMA is integrated with MISO-HBF (termed as MISO-NOMA-HBF) in this study for mmWave based cellular communication. Furthermore, the optimization of the analog precoder in the case of the HBF is a challenging issue [11-12]. Among different significant present works, analog beamforming has some difficulties due to its phase-shifter-based architecture [10-12]. In addition, analog precoders have a limited pre-defined codebook, hence manifold optimization, element-wise iterative algorithms, and analog beamformer optimization techniques have been proposed in previous research [10-11]. However, perfect CSI has been considered for those previous cases. Present studies on intelligent cellular communication have illustrated that the use of the deep learning (DL) technique is able to solve complex beamforming optimization for the users in the case of downlink MISO-HBF and imperfect CSI. Inspired by previous works, beamforming neural networks (BFNN) can optimize the analog precoder of the MISO-NOMA-HBF scheme depending on the imperfect CSI, channel condition, and the SINR of CEU to improve the user capacities as well as sum capacity (SC) [13]. The main contributions of this study are explained as follows:

- In this study, MISO-HBF is integrated with NOMA to provide multi-user access.
- MISO-NOMA-HBF is integrated with DL-based BFNN for CEU, which is termed as MISO-NOMA-HBF-BFNN to enhance the user capacities as well as SC for mmWave based B5G cellular communication.
- The user channel capacities and SC of the proposed MISO-NOMA-HBF-BFNN scheme are compared and evaluated with existing schemes (e.g., MISO-NOMA-HBF[13], and MISO-OMA-HBF-BFNN).
- The impacts of the different pilot to noise ratio (PNR) over the user capacities and SC of the proposed MISO-NOMA-HBF-BFNN scheme are also compared and evaluated with existing schemes [13].
- The effects of less accurate estimated channel paths over the user capacities and SC of the proposed scheme are also compared and evaluated with existing schemes as well [13].
- Using simulation results, the performance improvement of the proposed scheme compared to other existing schemes are explicitly analyzed.

2. System Model

A narrow band downlink (DL) MISO-NOMA-HBF-BFNN was considered on a mmWave system which illustrated in Fig. 1. HBF consists of digital and analog precoders. As observed in Fig. 1, a two user based single cell scenario was considered with a single base station as source (S). The S consists of one RF chain and N number of transmit antennae. The cell center user (CCU) is situated near the S, which is marked as UE_1. The cell edge user (CEU) is situated near the cell edge, is marked as UE_2 in Fig. 1. Moreover, d_1 and d_2 are the distance of UE_1 and UE_2 from S, simultaneously. The superimposed signal A is simultaneously transmitted towards the users, which is multiplied by a scalar digital precoder $\boldsymbol{v_D}$ and then by an $N \times 1$ analog precoder $\boldsymbol{v_{RF}}$ along with phase shifters. The precoded and superimposed signal ($A = \sqrt{p_1 P} x_1 + \sqrt{p_2 P} x_2$) can be represented by following equation:

$$\chi = \boldsymbol{v_{RF}} \boldsymbol{v_D} A, \tag{1}$$

Where x_1, and x_2 are the data symbols for UE_1 and UE_2, respectively. p_1 and p_2 represent the power allocation for UE_1, and UE_2, respectively. In addition, P is the total transmitted power from S, where

$p_1 + p_2 = 1$ and $p_1 < p_2$. To perform the optimization technique effectively, a self-defined lambda layer is included at the end of the BFNN optimization technique. Because of the 'sigmoid' activation function, $\boldsymbol{\alpha_2}$ symbolizes the real input value within the range (0,1) [13]. Therefore, the complex output value can be expressed by the following equation:

$$\boldsymbol{v_{RF}} = e^{j.2\pi\boldsymbol{\alpha_2}} = \cos(2\pi\boldsymbol{\alpha_2}) + j.sin(2\pi\boldsymbol{\alpha_2}), \tag{2}$$

where $j = \sqrt{-1}$, $2\pi\boldsymbol{\alpha_2}$ is corresponding to the phases of $\boldsymbol{v_{RF}}$. The superimposed signal is transmitted

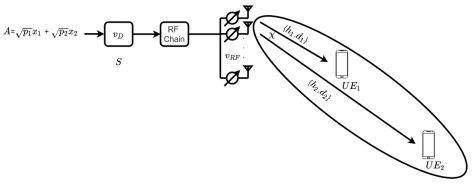

Figure 1. System model of proposed MISO-NOMA-HBF-BFNN scheme.

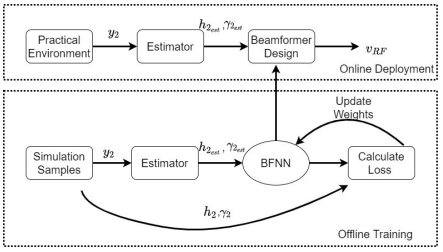

Figure 2. Principle of BFNN based MISO-NOMA-HBF for CEU.

through the MISO mmWave channel. Where h_k^H is the channel response between S and the respective user ($k\epsilon\{1,2\}$). A well-known Saleh-Valenzuela mmWave channel model, which was considered for h_k^H, consists of one line-of-sight (LOS) path and $L-1$ number of non line-of-sight (NLOS) paths. The channel response can be represented by the following equation [13-15]:

$$h_k^H = \sqrt{\frac{N}{L}} \sum_{l=1}^{L} \alpha_{k_l} a_l^H(\phi_t^l), \tag{3}$$

where α_l is the complex gain of the l^{th} path and $a_t(\phi_t^l)$ represents the antenna array response vector at S, with ϕ_t^l representing the departure azimuth angle related to the path l. $l = 1$ represents a LOS component in h_k^H. The received signal at UE_1 and UE_2 can be expressed by the following equations:

$$y_1 = h_1^H \boldsymbol{v_{RF}} \boldsymbol{v_D} A + n_1, \tag{4}$$

$$y_2 = h_2^H \boldsymbol{v_{RF}} \boldsymbol{v_D} A + n_2, \tag{5}$$

where n_k is the additive complex Gaussian noise that fulfills the circularly symmetric characteristics with covariance σ_k^2 and zero mean [13]. Since analog beamforming consists of analog phase shifters, a multi-layer

NN in which the network S is trained to UE_2 communication links is not a perfect solution [16-17]. A unique BFNN technique is considered for the channel between S and UE_2 of the proposed MISO-NOMA-HBF-BFNN scheme in this study. Because the path loss between S and UE_2 is higher than the path loss between S and UE_1 due to $d_1 < d_2$. This BFNN was considered to solve Eq. (9). The specific considerations and the design approach of the BFNN technique are given in below:

- BFNN Input: The BFNN is considered to train the S to the UE_2 link and generate an optimized analog BF vector ($\boldsymbol{v_{RF}}$) instead of training the entire communication link. Moreover, $h_{2_{est}}$ and $\gamma_{2_{est}}$ are fed as inputs to the considered BFNN technique for the proposed MISO-NOMA-HBF-BFNN scheme. Where $h_{2_{est}}$ is the estimated channel parameter from S to UE_2.

- Lambda layer: To perform the optimization technique effectively, a self-defined lambda layer is included at the end of the BFNN optimization technique. Because of the 'sigmoid' activation function, $\boldsymbol{\alpha_2}$ symbolizes the real input value within the range (0,1) [13]. Therefore, the complex output value can be expressed by the following equation:

$$\boldsymbol{v_{RF}} = e^{j.2\pi\boldsymbol{\alpha_2}} = \cos(2\pi\boldsymbol{\alpha_2}) + j.sin(2\pi\boldsymbol{\alpha_2}), \tag{6}$$

  where $j = \sqrt{-1}$, $2\pi\boldsymbol{\alpha_2}$ is corresponding to the phases of $\boldsymbol{v_{RF}}$.

- Loss function: The loss function due to the considered BFNN can be derived as follows [13]:

$$Loss = \frac{1}{M}\sum_{m=1}^{M}\log_2(1 + \frac{\gamma_{2_m}}{N}||h_{2_m}^H \boldsymbol{v_{RF,m}}||^2), \tag{7}$$

  Where M represents the total number of samples for training, and γ_{2m}, h_{2_m}, and $\boldsymbol{v_{RF,m}}$ represent the SINR, CSI, and output analog BF ($\boldsymbol{v_{RF}}$) associated with the m^{th} sample, respectively. The loss reduction is related to the increase of the average channel capacity of the UE_2 [13].

Based on the above considerations, the BFNN for UE_2 is shown in Fig. 2. The design approach consists of two stages. According to the system model, the channel samples are produced randomly during the offline training stage. Afterward, a practical mmWave channel estimation is performed to obtain the partial CSI at S. A traditional mmWave channel estimator was considered in this study. In this case, the S estimates the channel between S and UE_2 by transferring the beamformers along with pilot symbols as a hierarchical codebook. Furthermore, S receives the feedback from the decision of UE_2 based on y_2. SINR estimation $\gamma_{2_{est}}$ and the estimated channel of UE_2 ($h_{2_{est}}$) are then fed to the BFNN as inputs. $\gamma_2 = \gamma_{2_{est}}$ was considered in this study. Afterwards, the optimized $\boldsymbol{v_{RF,m}}$ are generated using the considered BFNN. The optimization is performed by minimizing the loss function. Furthermore, the SINR values and the channel samples were randomly generated by the simulation. The samples, along with the SINR values, are utilized to calculate the loss. Thus, the loss of UE_2 can be assured to converge according to the local optimal beamformer, as well as an appropriate learning rate. According to [13], the conventional channel estimation algorithm is utilized for obtaining $h_{2_{est}}$ based on the pilot signal. The pilot-to-noise power ratio (PNR) is assumed as as an indicator of the channel estimation level. Moreover, PNR is not same as SNR since the power of pilot signal and that of the data signal can be set to be different in practical systems. In the traditional HBF algorithms, h_2 is directly replaced by $h_{2_{est}}$ when calculating the BF coefficients. The channel estimation is treated as the input of the

BFNN considering a perfect CSI. Therefore, the BFNN is trained appropriately to deal with the ideal capacity with perfect CSI to determine the errors due to channel estimation.

The same channel estimation technique for the mmWave channel was used in the case of S during the online deployment stage. To achieve the optimized $\boldsymbol{v_{RF}}$, the estimated channel $h_{2_{est}}$ was then transferred to the BFNN. Perfect CSI is necessary at the offline training stage to calculate the loss. Every parameter of the considered BFNN for UE_2 should be properly set and the BFNN should be properly trained to deal with imperfect CSI, which is treated as an input and transferred directly to the output towards the analog beamformer during online deployment [13].

Table 1. Parameters of BFNN for CEU

Layer Name	Function	No. of Params.	O/P Dim.
Input Layer	\	0	129×1
Dense Layer 1	reLu	33024	256×1
Dense Layer 2	reLu	32896	128×1
Dense Layer 3	sigmoid	8256	64×1
Lambda Layer	\	0	64×1

In the case of the BFNN structure, a MISO system with $N = 64$ was considered, which is shown in Table. I. The detailed parameters of the BFNN, such as the layer name, output dimensions (O/P Dim.), activation function (Function), and trainable parameters of the individual layers (No. of Params.), are described in Table. I. According to Fig. 2, $h_{2_{est}}$ is fed into the input of the BFNN. However, the considered BFNN is a neural network which deals with real values only. Thus, the real part and the imaginary segment of $h_{2_{est}}$ are concatenated along with $\gamma_{2_{est}}$, which is also used as input for the BFNN. Moreover, $\gamma_{2_{est}}$ is an input vector with real values and dimension $(2N + 1) \times 1$. The dense layers of the BFNN were set to 256, 128, and 64 neurons, accordingly [13]. A batch normalized layer preceded each and every dense layer for convergence [13]. The Lambda layer performed the modulus operation on the final output of the BFNN. In this study, the training, testing, and validation sets contained 10^5, 10^4, and 10^4 samples, respectively [13].

3. Channel Capacity

3.1. Capacity of MISO-NOMA-HBF-BFNN

The signal to interference and noise ratio (SINR) of UE_1 and UE_2 are expressed as γ_1 and γ_2, respectively. γ_1 and γ_2 can be expressed as follows for the proposed scheme:

$$\gamma_1 = p_1 ||h_1^H \boldsymbol{v_{RF}} \boldsymbol{v_D}||^2 \rho, \tag{8}$$

$$\gamma_2 = \frac{p_2 ||h_2^H \boldsymbol{v_{RF}} \boldsymbol{v_D}||^2 \rho}{p_2 ||h_2^H \boldsymbol{v_{RF}} \boldsymbol{v_D}||^2 \rho + 1}, \tag{9}$$

Where $\rho = \frac{P}{\sigma^2}$ is the transmit signal-to-noise ratio (SNR). The channel capacity of UE_1 is expressed as C_1 and the channel capacity of UE_2 can be expressed as C_2. The user channel capacities can be expressed by the following equations:

$$C_1 = log_2(1 + \gamma_1), \tag{10}$$

$$C_2 = log_2(1 + \gamma_2), \tag{11}$$

The optimal value of $\boldsymbol{v_D}$ for maximizing C_2 is represented by $\sqrt{\frac{p_2}{N}}$. Afterwards, the HBF optimization problem for v_{RF} for UE_2 can be expressed as follows [13]:

$$\min_{v_{RF}} \log_2(1 + \frac{p_2||h_2^H \boldsymbol{v_{RF}} \boldsymbol{v_D}||^2 \frac{\rho}{N}}{p_2||h_2^H \boldsymbol{v_{RF}} \boldsymbol{v_D}||^2 \frac{\rho}{N} + 1}), \tag{12}$$

subjected to $|[\boldsymbol{v_{RF}}]_i|^2 = 1$ and $i = 1, ..., N$ [13]. In this study $\gamma_{2_{est}} = \gamma_2$ is assumed because the SINR can be estimated more accurately than the CSI. Where, $\gamma_{2_{est}}$ is the estimated SINR [13]. Furthermore, the SC (C_S) of the proposed MISO-MISO-NOMA-HBF-BFNN can be derived by adding C_1 and C_2 as in the following equation:

$$C_S = C_1 + C_2. \tag{13}$$

3.2. Capacity of MISO-OMA-HBF-BFNN

Time-division multiple access (TDMA) is considered for the MISO-OMA-HBF-BFNN. The MISO-OMA-HBF-BFNN scheme is described as a benchmark of the proposed MISO-NOMA-HBF-BFNN scheme to compare the user channel capacities and the SC. S transmits the information signal towards UE_1 and UE_2 individually in various independent time slots along with P in this case without any interference. Where, P represents the total transmit power from S. Thus, in the case of TDMA based MISO-OMA-HBF-BFNN, independent time slots are allocated for the users to transmit individual symbols (e.g., x_1, and x_2). Two different independent time slots are denoted as t_1, and t_2 to transmit x_1 and x_2 towards UE_1 and UE_2, respectively [13,16]. Hence, equally divided time slots ($t_1 = t_2 = \frac{1}{2}$) are considered here. Thus, the achievable capacity of UE_1, UE_2, and the SC can be presented as follows for the MISO-OMA-HBF-BFNN scheme:

$$C_1^{OMA} = \frac{1}{2} log_2(1 + \gamma_1^{OMA}), \tag{14}$$

$$C_2^{OMA} = \frac{1}{2} log_2(1 + \gamma_2^{OMA}), \tag{15}$$

Where $\gamma_1^{OMA} = ||h_1^H v_{RF} v_D||^2 \rho$ and $\gamma_2^{OMA} = ||h_2^H v_{RF} v_D||^2 \rho$. Moreover, the optimal v_D for enhancing C_2 is expressed by $\sqrt{\frac{P}{N}}$. Then, the optimization problem for v_{RF} due to MISO-OMA-HBF-BFNN for UE_1 and UE_2 can be expressed as follows by [13]:

$$\min_{v_{RF}} \log_2(1 + ||h_1^H v_{RF}||^2 \frac{\rho}{N}), \tag{16}$$

$$\min_{v_{RF}} \log_2(1 + ||h_2^H v_{RF}||^2 \frac{\rho}{N}), \tag{17}$$

subject to $|[v_{RF}]_i|^2 = 1$, for $i = 1, ..., N$. As the SINR can be estimated more accurately than the CSI, hence $\gamma_{1_{est}}^{OMA} = \gamma_1^{OMA}$ and $\gamma_{2_{est}}^{OMA} = \gamma_2^{OMA}$ are assumed in this study. Where $\gamma_{1_{est}}^{OMA}$ and $\gamma_{2_{est}}^{OMA}$ are the estimated SINR [13]. Furthermore, the SC of MISO-OMA-HBF-BFNN can be derived by adding C_1^{OMA} and C_2^{OMA} as in the following equation:

$$C_S^{OMA} = C_1^{OMA} + C_2^{OMA}. \tag{18}$$

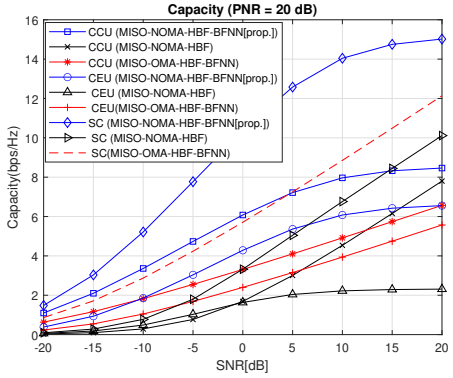

Figure 3. Capacity comparisons for PNR = 20 dB and $L_{est} = 3$.

4. Simulation Results

For simulation purposes, a MISO based array antenna with $N = 64$ and uniform linear half-wave spacing was considered at S. The Saleh-Valenzuela based mmWave channel model was considered for all communication links in this study. Parameters $p_1 = 0.2$, $p_2 = 1 - p_1$, $P = 1$, and $L = 3$ were considered in this study. The pilot-to-noise ratio (PNR) was considered as an indicator of the channel estimation because PNR and SNR cannot be the same in practical scenarios [13]. The details of the BFNN parameters were set as listed in Table. I. The same parameters were used for the other compared schemes. The Adam optimizer was considered in this study. In the considered BFNN, the hyper-parameter setting is shown in Table I and remain constant throughout all experiments. The learning rate is initialized at 0.001 and the Adam optimizer is utilized in the proposed scheme. To assure the effectiveness of the SNR, the training samples were considered within -20 dB to 20 dB and imperfect CSI was also considered for all comparisons [13].

Fig. 3 illustrates the capacity comparisons for the proposed scheme and the other compared schemes in the case of $PNR = 20dB$ and the estimated channel paths, $L_{est} = 3$. The proposed scheme provides significantly higher user capacities than other compared scheme. Because due to the proposed BFNN technique for MISO-NOMA-HBF-BFNN scheme, the analog beamformer $\boldsymbol{v_{RF}}$ is optimized based on h_{2est} and $\gamma_{2_{est}}$. Hence. the CCU (UE_1) and CEU (UE_2) capacities are significantly improved for the proposed scheme compared to other schemes. Thus, SC is also improved by the proposed scheme compared to other schemes which is illustrated in Fig. 3.

Fig. 4 illustrates the CCU capacity comparisons for the proposed MISO-NOMA-HBF-BFNN scheme and the other existing schemes under $PNR = 0dB$ and $L_{est} = 3$. The proposed scheme provides significantly higher user capacities than other compared schemes in the case of $PNR = 0dB$. Due to the considered BFNN technique for MISO-NOMA-HBF-BFNN scheme, the analog beamformer $\boldsymbol{v_{RF}}$ is optimized based on $h_{2_{est}}$ and $\gamma_{2_{est}}$. Hence. the CCU and CEU capacities are significantly improved for the proposed scheme compared to other schemes in the case of lower PNR. Thus, SC is also improved in case of the proposed scheme which is also illustrated in Fig. 4. However, the capacities are decreased in the case of PNR = $0dB$ compared to PNR = $20dB$ due to the low PNR in the case of the proposed MISO-NOMA-HBF-BFNN scheme which is shown in Fig. 4.

Fig. 5 shows that the channel capacity comparisons for the proposed MISO-NOMA-HBF-BFNN scheme and the other compared schemes in the case of $PNR = 20dB$ and $L_{est} = 1$. In Figure 5, the proposed scheme provides remarkably greater user channel capacities and SC compared to the other conventional schemes in the

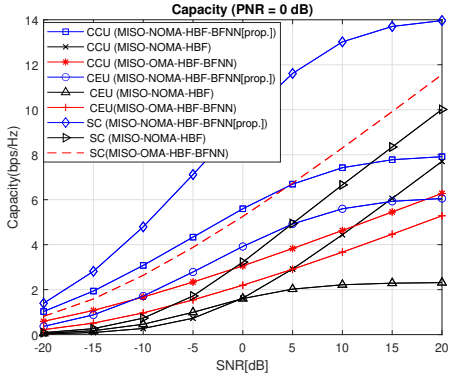

Figure 4. Capacity comparisons for PNR = 0 dB and $L_{est} = 3$.

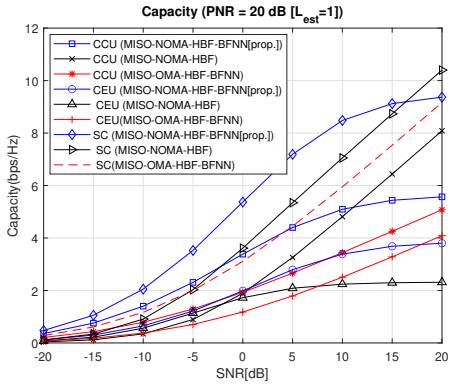

Figure 5. SC comparisons for PNR = 20 dB and $L_{est} = 1$.

case of lower SNR. In contrast, the capacities are degraded in the case of the proposed scheme due to higher SNR compared to conventional MISO-NOMA-HBF. Because the proposed BFNN can optimize the analog beamformer $\boldsymbol{v_{RF}}$ effectively in case of lower SNR due to less accurate channel path (L_{est}). Due to higher SNR, the proposed BFNN cannot optimize the analog beamformer $\boldsymbol{v_{RF}}$ effectively and cannot provide higher user channel capacities as well as SC due to less accurate L_{est}. However, the capacities are decreased in the case of $L_{est} = 1$ compared to $L_{est} = 3$ due to the less accurate L_{est} in the case of the proposed MISO-NOMA-HBF-BFNN scheme which is illustrated in Fig. 5 as well.

5. Conclusion

In this study, the MISO-NOMA-HBF-BFNN scheme is proposed for mmWave based downlink MISO-NOMA B5G cellular communication. The performance of the MISO-NOMA-HBF-BFNN scheme is analyzed extensively in terms of user channel capacities and SC. Moreover, the user channel capacities and SC of the proposed scheme are also compared with the conventional MISO-NOMA-HBF and MISO-OMA-HBF-BFNN schemes. The result analysis illustrates that, due to the proposed scheme, the CCU channel capacity, CEU channel capacity and SC are improved compared to the other compared schemes due to the BFNN for CEU due to imperfect CSI. Because the analog beamformer can effectively be optimized by the BFNN for CEU due to the imperfect CSI. Thus, the user channel capacities and SC of the proposed MISO-NOMA-HBF-BFNN scheme are improved

compared to other existing schemes. The impact of different PNR and L_{est} are also analyzed for the proposed scheme and compared with other existing schemes. The result analysis also illustrated that the proposed scheme outperforms other existing schemes in terms of user capacities and SC in the case of different PNR and L_{est} as well.

References

[1] M. F. Kader and S. Y. Shin, "Cooperative Relaying Using Space-Time Block Coded Non-orthogonal Multiple Access," in IEEE Transactions on Vehicular Technology, vol. 66, no. 7, pp. 5894-5903, July 2017.

[2] A. A. Amin and S. Y. Shin, "Channel Capacity Analysis of Non-orthogonal Multiple Access with OAM-MIMO System," in IEEE Wireless Communications Letters, Early Access.

[3] J. W. Kim, S. Y. Shin, and V. C. M. Leung, "Performance Enhancement of Downlink NOMA by Combination With GSSK," IEEE Wireless Communications Letters, vol. 7, no. 5, pp. 860–863, 2018.

[4] Z. Wei, D. W. K. Ng and J. Yuan, "NOMA for Hybrid mmWave Communication Systems With Beamwidth Control," in IEEE Journal of Selected Topics in Signal Processing, vol. 13, no. 3, pp. 567-583, June 2019

[5] Z. Chen, Z. Ding, X. Dai and G. K. Karagiannidis, "On the Application of Quasi-Degradation to MISO-NOMA Downlink," in IEEE Transactions on Signal Processing, vol. 64, no. 23, pp. 6174-6189, Dec.1, 2016.

[6] Z. Chen, Z. Ding, P. Xu and X. Dai, "Optimal Precoding for a QoS Optimization Problem in Two-User MISO-NOMA Downlink," in IEEE Communications Letters, vol. 20, no. 6, pp. 1263-1266, June 2016.

[7] Y. Jeong, C. Lee and Y. H. Kim, "Power Minimizing Beamforming and Power Allocation for MISO-NOMA Systems," in IEEE Transactions on Vehicular Technology, vol. 68, no. 6, pp. 6187-6191, June 2019.

[8] J. Zhang, Y. Zhu, S. Ma, X. Li and K. Wong, "Large System Analysis of Downlink MISO-NOMA System via Regularized Zero-Forcing Precoding with Imperfect CSIT," in IEEE Communications Letters.

[9] A. Alkhateeb, O. El Ayach, G. Leus and R. W. Heath, "Channel estimation and hybrid precoding for millimeter wave cellular systems", IEEE J. Sel. Topics Signal Process., vol. 8, no. 5, pp. 831-846, Oct. 2014.

[10] T. Lin, J. Cong, Y. Zhu, J. Zhang and K. B. Letaief, "Hybrid beamforming for millimeter wave systems using the MMSE criterion", IEEE Trans. Commun., vol. 67, no. 5, pp. 3693-3708, May 2019.

[11] X. Yu, J.-C. Shen, J. Zhang and K. B. Letaief, "Alternating minimization algorithms for hybrid precoding in millimeter wave MIMO systems", IEEE J. Sel. Topics Signal Process., vol. 10, no. 3, pp. 485-500, Apr. 2016.

[12] F. Sohrabi and W. Yu, "Hybrid digital and analog beamforming design for large-scale antenna arrays", IEEE J. Sel. Topics Signal Process., vol. 10, no. 3, pp. 501-513, Apr. 2016.

[13] T. Lin and Y. Zhu, "Beamforming Design for Large-Scale Antenna Arrays Using Deep Learning," in IEEE Wireless Communications Letters, vol. 9, no. 1, pp. 103-107, Jan. 2020.

[14] X. Gao, L. Dai, S. Han, C.-L. I and X. Wang, "Reliable beamspace channel estimation for millimeter-wave massive MIMO systems with lens antenna array", IEEE Trans. Wireless Commun., vol. 16, no. 9, pp. 6010-6021, Sep. 2017.

[15] H. He, C.-K. Wen, S. Jin and G. Y. Li, "Deep learning-based channel estimation for beamspace mmWave massive MIMO systems", IEEE Wireless Commun. Lett., vol. 7, no. 5, pp. 852-855, Oct. 2018.

[16] Z. Qin, H. Ye, G. Y. Li and B.-H. F. Juang, "Deep learning in physical layer communications", IEEE Wireless Commun., vol. 26, no. 2, pp. 93-99, Apr. 2019.

[17] H. Ye, G. Y. Li and B.-H. Juang, "Power of deep learning for channel estimation and signal detection in OFDM systems", IEEE Wireless Commun. Lett., vol. 7, no. 1, pp. 114-117, Feb. 2018.